PROCEEDINGS OF SCIENCE

Wgamma and Zgamma Production in 7 TeV pp collisions

Syue-Wei Li*
On behalf of the CMS Collaboration
National Central University, Taiwan
E-mail: Syue-Wei.Li@cern.ch

We present the measurements of $W\gamma$ and $Z\gamma$ production using data corresponding to the full 2010 and 2011 periods of the LHC run. For charged lepton decay modes of W and Z bosons the total cross sections are measured for photon transverse energy greater than 10 GeV. The results are also interpreted in terms of limits of anomalous trilinear gauge couplings (aTGCs). We also present the first measurement of $Z\gamma$ production using the $\nu\nu\gamma$ final state for photon transverse energy greater than 145 GeV.

36th International Conference on High Energy Physics,
July 4-11, 2012
Melbourne, Australia

*Speaker.

PoS(ICHEP2012)084

1. Introduction

The self-interaction among the gauge bosons in the standard model (SM) is a direct consequence of the non-Abelian symmetry. As such, the triple and quartic gauge coupling constants (TGC and QGC) are completely fixed in the SM by the gauge structure of the $SU(2) \times U(1)$. The study of diboson production in proton-proton collisions allows stringent tests in the electroweak sector of the SM at the LHC.

We present the measurement of the $W\gamma$ and $Z\gamma$ cross sections, and of the $WW\gamma$, $ZZ\gamma$, and $Z\gamma\gamma$ triple gauge coulings with charged lepton decay channel at $\sqrt{s}$ = 7 TeV, using data collected with the CMS detector, corresponding to an integrated luminosify of 36 pb^{-1} [1]. The first result of $Z\gamma$ in neutrino channel based on data corresponding to an integrated luminosify of 5 fb^{-1} is presented as well [2]. A complete description of the CMS detector and information about objects reconstruction can be found in Ref. [3].

2. Measurements of $W\gamma$ and $Z\gamma$ production

2.1 $W\gamma$ and $Z\gamma$ cross sections in charged leptonic channel

The $W\gamma \to \ell\gamma$ (ℓ = e, μ) final state is characterized by a prompt, energetic, and isolated lepton, significat missing transverse energy (E_T^{miss}) due to a neutrino from W boson decay, and a prompt isolated photon. The $Z\gamma \to \ell\ell\gamma$ final state has two isolated leptons and a prompt isolated photon. Events are selected by a trigger that requires at least one energetic lepton. As the cross section diverges for soft photons or those that are spatially close to charged lepton, we restrict our measurement to the phase space defined by photon E_T > 10 GeV and $\Delta R(\ell,\gamma) > 0.7$. Furthermore, the E_T^{miss} should be larger than 25 GeV for $W\gamma \to \ell\gamma$, and the invariant mass of the two lepton candidates ($M_{\ell\ell}$) must be larger than 50 GeV for $Z\gamma \to \ell\ell\gamma$. We require isolated lepton to have p_t > 20 GeV and $|\eta| < 2.5$ (2.4 for muon). The muon candidates in $W\gamma \to \mu\gamma$ are further restricted to be in $|\eta| < 2.1$. We require a well identified and isolated photon in $|\eta| < 1.44$ or $1.57 < |\eta| < 2.5$.

The main background to $W\gamma$ and $Z\gamma$ production consists of W+jets and Z+jets events, respectively, where the photon candidate originates from one of the jets. We estimate this background from data by measuring the E_T-dependent probability for a jet is misidentifed as photon, and then folding this probability with the non-isolated photon candidate E_T spectrum observed in the $W\gamma$ and $Z\gamma$ samples. The estimation of the backgroud from misidentified jets for the $W\gamma$ and $Z\gamma$ processes is further cross-checked with W+jets and Z+jets MC simulation and the result with obtained from an independent study of photon cluster shower shape following the same approach as in Ref. [4]. We observe good agreement between all three methods (shown in Figure 1).

For $W\gamma$ analysis, backgrounds from other sources, such as $Z\gamma$ where one of the leptons from Z boson decay does not pass reconstruction and identification criteria and diboson processes where one of the electrons is misidentified as a photon, are estimated from MC simulation. The $W\gamma \to \tau\nu\gamma$ production, with subsequent $\tau \to \ell\nu\nu$ decay, also contributes at the few percent level. We rely on MC simulation to estimate this contribution.

For $Z\gamma$ analysis, other backgrounds from multijet QCD, γ+jets, $t\bar{t}$, and other diboson processes contribute less than one event in each of the two channels and are therefore neglected in this analysis.

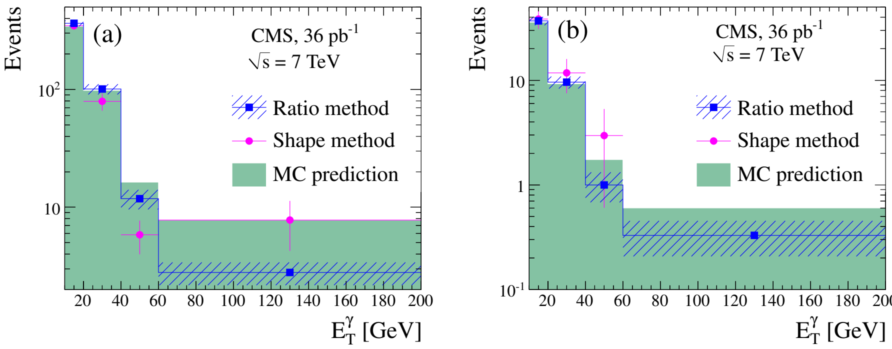

Figure 1: Background from misidentified jets as a function of the photon candidate E_T, estimated from the ratio method, is shown with blue squares together with an alternative method that uses energy deposition shape templates (magenta circles), and MC simulation (green filled histogram) for (a) $W\gamma$ and (b) $Z\gamma$ channels. Uncertainties include both statistical and systematic sources.

The photon E_T distribution passing the full event selection is given in Figure 2. The distribution of the $\ell\ell\gamma$ mass as a function of the dilepton mass is displayed in Figure 2. We observe good agreement between data and the SM prediction.

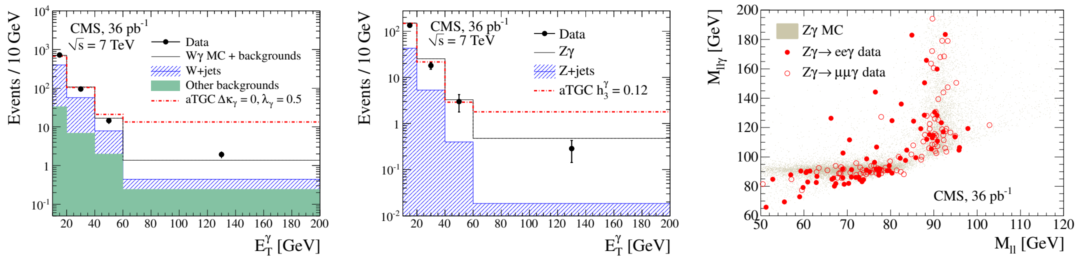

Figure 2: Transverse energy distribution for the photon candidates for $W\gamma$ (left) and $Z\gamma$ (middle) production. Data are shown with black circles with error bars; expected signal plus background is shown as a black solid histogram; the contribution from misidentified jets is given as a hatched blue histogram, and the background from γ+jets, $t\bar{t}$, and multiboson processes is given as a solid green histogram. A typical aTGC signal is given as a red dot-and-line histogram. The last bin includes overflows. Entries in wider bins are normalized to the ratio of 10 GeV and the bin width. Distribution of the $\ell\ell\gamma$ invariant mass as a function of the dilepton invariant mass for selected $Z\gamma$ candidates (right) in the electron (filled circles) and muon (open circles) final states. The data accumulation at $M_{\ell\ell\gamma} \simeq M_Z$ corresponds to FSR events, while the data at $M_{\ell\ell} \simeq M_Z$ correspond to ISR events.

The measured cross section of $W\gamma$ is $\sigma(\mathrm{pp} \to W\gamma + X) \times \mathscr{B}(W \to \ell\nu) = 56.3 \pm 5.0$ (stat.) $\pm$ 5.0 (syst.) $\pm$ 2.3 (lumi.) pb. This result agrees well with the NLO prediction [5] of 49.4 ± 3.8 pb with $E_T^\gamma > 10$ GeV and $\Delta R(\ell, \gamma) > 0.7$. The measured cross section of $Z\gamma$ is $\sigma(\mathrm{pp} \to Z\gamma + X) \times \mathscr{B}(Z \to \ell\ell) = 9.4 \pm 1.0$ (stat.) $\pm$ 0.6 (syst.) $\pm$ 0.4 (lumi.) pb. The theoretical NLO prediction [6] for $E_T^\gamma >$ 10 GeV, $\Delta R(\ell, \gamma) > 0.7$ and $M_{\ell\ell} > 50$ GeV is 9.6 ± 0.4 pb, which is in agreement with the measured value.

2.2 Anomalous triple gauge couplings

Limits on anamolous triple gauge couplings have been set based on photon E_T spectrum. The corresponding deviation is modelled by an effective Lagrangien built without form factor and requiring CP invariance. In $W\gamma$ analysis limits are extracted on $\Delta\kappa_\gamma$ and λ_γ couplings associated to $WW\gamma$ vertex. In $Z\gamma$ analysis limits are extracted on h_i^Z and h_i^γ (i = 3, 4) couplings related to $ZZ\gamma$ and $Z\gamma\gamma$ vertices. The resultant two-dimentional 95% confidence level (CL) limits are given in Figure 3. To set one-dimensional 95% CL limits on a given anomalous coupling we set the other aTGCs to their respective SM predictions. The results are summarized in Table 2.2.

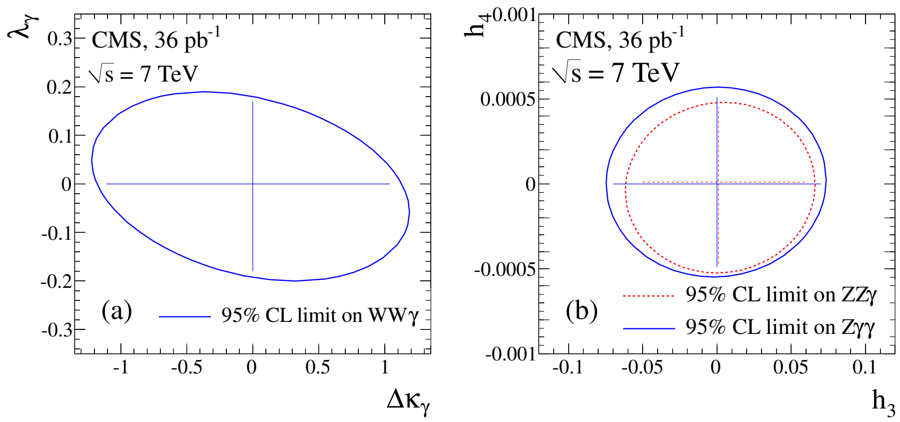

Figure 3: Two-dimensional 95% CL limit contours (a) for the WWγ vertex couplings λ_γ and $\Delta\kappa_\gamma$ (blue line), and (b) for the ZZγ (red dashed line) and Z$\gamma\gamma$ (blue solid line) vertex couplings h_3 and h_4 assuming no energy dependence on the couplings. One-dimensional 95% CL limits on individual couplings are given as solid lines.

WWγ	ZZγ	Z$\gamma\gamma$
$-1.11 < \Delta\kappa_\gamma < 1.04$	$-0.05 < h_3 < 0.06$	$-0.07 < h_3 < 0.07$
$-0.18 < \lambda_\gamma < 0.17$	$-0.0005 < h_4 < 0.0005$	$-0.0005 < h_4 < 0.0006$

Table 1: One dimensional 95% CL limits on WWγ, ZZγ, and Z$\gamma\gamma$ aTGCs.

3. $Z\gamma$ in neutrino channel

The $Z\gamma \to \nu\bar{\nu}\gamma$ final state is characterized by significat E_T^{miss}, and a prompt isolated photon. The data is selected from events that pass a single-photon trigger that is fully efficient within the signal region of $|\eta| < 1.44$ and $E_T > 145$ GeV. Furthermore, E_T^{miss} requirement is optimized to be greater than 130 GeV. Events with excessive hadronic activity are removed by requiring that there are no particle flow jets [7], and that there are no tracks outside of $\Delta R(track, \gamma) = 0.04$ with pT > 20 GeV.

Backgrounds unrelated to pp collisions are removed by further cuts. Protons that stray from the beam, can shower to muons that bremsstrahlung in the ECAL. These and showers from cosmic muons are reduced by vetoing muon tracks and requiring that the time assigned to the photon is ±3 ns of that expected of a collision particle's arrival at the ECAL. Other anomalous ECAL signals are reduced by requiring that the timing of all the deposits comprising the photon are consistent. Any backgrounds unrelated to pp collisions remaining are estimated from data by examining the transverse distribution of energy in the EM cluster and the time of arrival of the signal in the channel with the largest energy deposition. It is found that only the halo muons give a significant residual contribution to the in-time sample.

Events of $W \to e\nu$ can mimic the monophoton signal, if the electron is misreconstructed. Estimating with MC simulated events and verifying with $Z \to ee$ events in data shows that the matching of electron showers to pixel seeds has an efficiency of $\varepsilon = 0.9940 \pm 0.0025$. The contribution of $W \to e\nu$ events in the sample is found by scaling a control sample of electron candidates by (1-ε)/ε.

The contamination from jets misidentified as photons is estimated by using a control sample of EM-enriched QCD events to calculate the ratio of events that pass the signal photon criteria relative to those that pass photon criteria but fail an isolation requirement. Since the EM-enriched sample also includes the prompt photons, this additional contribution to the ratio is estimated by fitting templates of cluster shower shape from MC-simulated γ+jets events to an independent QCD data sample. This contribution of prompt photons is subtracted from the numerator of the ratio. This corrected ratio is applied to the non-isolated photon candidate E_T spectrum observed in $Z\gamma \to \nu\bar{\nu}\gamma$ sample. The irreducible background, γ+jets, $W \to \ell\nu$, and diphoton backgrounds are estimated using MC simulation.

The results are summarized in Table 3. Observation is consistent with the SM prediction.

Process	Events
$Z\gamma \to \nu\bar{\nu}\gamma$	45.3 ± 6.9
Non-collision background	11.1 ± 5.6
$W \to e\nu$	3.5 ± 1.5
Jets misidentified as photons	11.2 ± 2.8
Others (γ+jets, etc)	4.1 ± 1.0
Total SM, includes $Z\gamma \to \nu\bar{\nu}\gamma$	75.1 ± 9.5
Data	73

Table 2: Summary of events from each process for 5 fb^{-1}.

4. Summary

We performed the measurement of $W\gamma$ and $Z\gamma$ corss sections with charged lepton decay using 36 pb^{-1} of pp collision at $\sqrt{s}$ = 7 TeV for $E_T^{\gamma} > 10$ GeV and $\Delta R(\ell,\gamma) > 0.7$, and additional requirement on the dilepton invariant mass to exceed 50 GeV for $Z\gamma$ process. We measured the $W\gamma$ cross section times the branching fraction for the leptonic W decay to be $\sigma(\mathrm{pp} \to W\gamma+X) \times \mathscr{B}(W \to \ell\nu)$ = 56.3 $\pm$ 5.0 (stat.) $\pm$ 5.0 (syst.) $\pm$ 2.3 (lumi.) pb. This result is in good agreement with the NLO prediction of 49.4 ± 3.8 pb, where the uncertainty includes both PDF and k-factor uncertainties. The $Z\gamma$ cross section times the branching fraction for the leptonic Z decay was measured to be

$\sigma(\text{pp} \to Z\gamma + X) \times \mathscr{B}(Z \to \ell\ell)$ = 9.4 $\pm$ 1.0 (stat.) $\pm$ 0.6 (syst.) $\pm$ 0.4 (lumi.) pb, which also agrees well with the NLO predicted value of 9.6 ± 0.4 pb. We also searched and found no evidence for anomalous WWγ, ZZγ, and Z$\gamma\gamma$ trilinear gauge couplings. We set the 95% CL limits on these couplings at $\sqrt{s} = 7$ TeV.

We also performed a first measurement of $Z\gamma \to \nu\bar{\nu}\gamma$ using 5 fb^{-1} of pp collision at $\sqrt{s}$ = 7 TeV. Observation agrees with the SM prediction.

References

[1] The CMS collaboration, *Measurement of $W\gamma$ and $Z\gamma$ production in pp collisions at $\sqrt{s}$ = 7 TeV*, Phys. Lett. B, **701**, 535-555 (2011).

[2] The CMS collaboration, *Search for Dark Matter and Large Extra Dimensions in pp Collision Yielding a Photon and Missing Transverse Energy*, Phys. Rev. Lett., **108**, 261803 (2012).

[3] The CMS collaboration, *The CMS experiment at the CERN LHC*, JINST 3 (2008) S08004.

[4] The CMS collaboration, *Measurement of the Isolated Prompt Photon Production Cross Section in pp Collisions at $\sqrt{s}$ = 7 TeV*, Phys. Rev. Lett., **106**, 082001 (2011).

[5] U. Baur, T. Han, and J. Ohnemus, *QCD corrections to hadronic $W\gamma$ production with nonstandard $WW\gamma$ couplings*, Phys. Rev., **D48** 5140 (1993).

[6] U. Baur, and E. Berger, *Probing the weak-boson sector in $Z\gamma$ production at hadron colliders*, Phys. Rev., **D47** 4889 (1993).

[7] The CMS collaboration, *Particle-flow commissioning with muons and electrons from J/Psi, and W events at 7 TeV*, CMS-PAS-JME-2010-005 (2010).

PoS(ICHEP2012)084